Hindawi
Oxidative Medicine and Cellular Longevity
Volume 2020, Article ID 8956504, 14 pages
https://doi.org/10.1155/2020/8956504

Research Article

Mitochondrial Dysfunctions May Be One of the Major Causative Factors Underlying Detrimental Effects of Benzalkonium Chloride

Anton G. Rogov,[1] Tatyana N. Goleva,[1] Evgeniya I. Sukhanova,[1] Khoren K. Epremyan,[1] Tatiana A. Trendeleva,[1] Alexandra P. Ovchenkova,[1] Dinara A. Aliverdieva,[2] and Renata A. Zvyagilskaya[1]

[1]*Federal Research Center "Fundamentals of Biotechnology", Russian Academy of Sciences, Leninsky pr. 33, 119071 Moscow, Russia*
[2]*Caspian Institute of Biological Resources of the Russian Academy of Sciences, M. Gadzhiev st. 45, Makhachkala, 367025, Russia*

Correspondence should be addressed to Renata A. Zvyagilskaya; renata_z@inbi.ras.ru

Received 24 September 2019; Revised 23 December 2019; Accepted 10 January 2020; Published 10 February 2020

Academic Editor: Ryuichi Morishita

Benzalkonium chloride (BAC) is currently the most commonly used antimicrobial preservative in ophthalmic solutions, nasal sprays, and cosmetics. However, a large number of clinical and experimental investigations showed that the topical administration of BAC-containing eye drops could cause a variety of ocular surface changes, from ocular discomfort to potential risk for future glaucoma surgery. BAC-containing albuterol may increase the risk of albuterol-related systemic adverse effects. BAC, commonly present in personal care products, in cosmetic products can induce irritation and dose-dependent changes in the cell morphology. The cationic nature of BAC (it is a quaternary ammonium) suggests that one of the major targets of BAC in the cell may be mitochondria, the only intracellular compartment charged negatively. However, the influence of BAC on mitochondria has not been clearly understood. Here, the effects of BAC on energy parameters of rat liver mitochondria as well as on yeast cells were examined. BAC, being a "weaker" uncoupler, potently inhibited respiration in state 3, diminished the mitochondrial membrane potential, caused opening of the Ca2+/Pi-dependent pore, blocked ATP synthesis, and promoted H_2O_2 production by mitochondria. BAC triggered oxidative stress and mitochondrial fragmentation in yeast cells. BAC-induced oxidative stress in mitochondria and yeast cells was almost totally prevented by the mitochondria-targeted antioxidant SkQ1; the protective effect of SkQ1 on mitochondrial fragmentation was only partial. Collectively, these data showed that BAC acts adversely on cell bioenergetics (especially on ATP synthesis) and mitochondrial dynamics and that its prooxidant effect can be partially prevented by the mitochondria-targeted antioxidant SkQ1.

1. Introduction

Benzalkonium chloride (BAC) (its chemical structure is shown in Figure 1) is a synthetic quaternary ammonium compound with amphoteric surface-acting properties [1]. It is a mixture of several alkyldimethylbenzylammonium chlorides differing only in the length of their alkyl side chains; commercially available BAC consists of benzyldodecyldimethylammonium chloride, benzyldimethyltetradecylammonium chloride, and benzylcetyldimethylammonium chloride [2]. BAC, a membrane-active cationic surfactant, is remarkable by its stability, high water solubility, low cost, and superior biocidal activity against most bacteria, fungi, algae, and some viruses [3–6]. It is extensively employed as an antimicrobial in hospitals, agriculture, and the food industry [4], in ophthalmic preparations [7], nasal sprays [8], multidose albuterol nebulizer solutions [9, 10], as a skin disinfectant and hand sanitizer [11], in cosmetics, numerous toothpastes and mouth rinses, lozenges, and dental restoratives [12–16].

The mechanism of antimicrobial action of BAC is still unknown in detail, but there is concern that biocide effect may occur through ionic and hydrophobic interactions, the increased expression of efflux pumps with the subsequent leakage of intracellular constituents, ultimately leading to cell death [2, 17]. The BAC-mediated surplus of ROS might lead

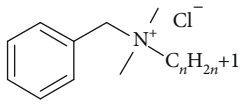

$n = 8, 10, 12, 14, 16, 18$

Figure 1: Structure of BAC.

to DNA damage and a decrease in glutathione, suggesting an apoptotic phenomenon [18]. The mechanism of action of BAC on fungal cells, including yeasts, is believed to be similar to the antibacterial activity [17]. It should, however, be recognized that only limited work has been dedicated to assess this issue, which remains not clearly understood.

Although BAC provides excellent antimicrobial properties in ophthalmic preparations, a large number of clinical and experimental investigations using *in vitro* or animal models suggested cytotoxic effects of even low BAC concentrations on several components of the eye (see [18]). The topical administration of BAC-containing eye drops may cause a variety of ocular surface changes, from ocular discomfort, redness, dryness, and tear film instability [19–26] to allergic, immune, inflammatory reactions [27–29], ocular irritation, scarring of the ocular surface with irreversible vision impairment [21, 30, 31], disruption of the blood-aqueous barrier inducing cystoid macular edema following cataract surgery [32, 33], loss of goblet cells (see [27, 34]) and, at higher concentrations, to the disruption of the corneal epithelium, induction of apoptosis or necrosis of Chang's conjunctival cells [31–33, 35, 36]. The proapoptotic effects were seen at very low concentrations of BAC with a threshold of toxicity found at about 0.005% (i.e., below the usual concentration used in most eye drops). In addition, ROS production in preserved formulations was at significantly higher levels than those observed with unpreserved drugs [31].

BAC added to the multidose albuterol nebulizer solution as an antimicrobial produced bronchospasm that was dose-dependent and cumulative [37]. Moreover, the use of BAC-containing albuterol during severe acute asthma exacerbations may antagonize the bronchodilator response to albuterol and increase the risk of albuterol-related systemic adverse effects [9].

Long-term use of intranasal corticosteroids with BAC can lead to high-grade dysplasia in the nasal mucosa [38].

BAC, commonly present as a preservative in personal care and cosmetic products, can induce irritation, predisposal to sensitization in dermatitis patients [39–41], dose-dependent changes in the cell morphology, and at higher concentrations neural toxicity through ROS induction and apoptosis [12], and even cell atrophy [13].

At the cellular level, in neuroblastoma cells [42] and the mouse neonatal brain [43], BAC exposure significantly modified lipid homeostasis changing several lipid classes. Long-term exposure of *Escherichia coli* to environmentally relevant BAC concentrations resulted in significant alterations in global gene expression with increasing the expression of genes associated with efflux and reducing the expression of genes associated with outer-membrane porins, motility, and chemotaxis [44]. In cultured human alveolar epithelial cells, BAC induced a dose- and concentration-dependent oxidative stress [45]. At high concentrations, BAC brought about neural toxicity in rat brains through ROS induction and apoptosis [12].

However, the cationic nature of BAC (it is a quaternary ammonium) suggests that one of the major targets of BAC in the cell may be mitochondria, the only intracellular compartment charged negatively. Indeed, a short-term exposure of Chang's conjunctival cells to BAC at concentrations ranging between 0.0001% and 0.01% significantly decreased the fluorescent intensity of Rhodamine 123, a membrane potential-related fluorescent probe, suggesting partial mitochondrial dysfunction, supposedly due to the opening of mitochondrial permeability transition pores; simultaneously, an enhanced hydrogen peroxide production was observed under these conditions [32]. In mice having a mutated mitochondrial complex II (succinate dehydrogenase) of the respiratory chain with overproduction of superoxide anion radicals, mitochondria-induced oxidative stress can be a causative factor for the development of dry eye disease [46]. Moreover, mitochondrial oxidative stress can influence pathogenesis and progression of age-related corneal diseases, as well as generalized corneal aging [47]. BAC at pharmacologically relevant concentrations inhibited mitochondrial ATP production and oxygen consumption in human corneal epithelial cells and cells bearing LHON mutations and osteosarcoma cybrid cells, possibly by directly targeting mitochondrial complex I [48, 49]. The authors concluded that the findings obtained support the urgent need for additional research on the mitochondria-related inhibitory effects of BAC [49]. Since mitochondria play a pivotal role in cellular functions, exact identification of molecular targets of BAC in mitochondria may greatly assist in a better understanding of biochemical mechanisms underlying its adverse effects.

In this study, we comprehensively analyzed BAC effects on energy parameters of isolated tightly coupled rat liver mitochondria, which are a perfect model for such kind of these investigations as they combine relative simplicity of their isolation with obtaining sufficient amounts of high-quality organelles. Other model organisms used in this study were yeasts *Yarrowia lipolytica* and *Dipodascus magnusii* with the respiratory chains closely resembling those of higher organisms [50, 51]. The *Y. lipolytica* yeast, an obligate aerobe amenable to both classical and molecular genetic techniques, and the *D. magnusii* giant cells containing branched mitochondrial network (see [52]) are exceptionally useful models for deciphering effects exerted by biologically active compounds on cell metabolism and mitochondrial dynamics. The benefits of humanized yeast models to provide insight into the mechanisms of key biochemical processes have been repeatedly documented (see [53–57]).

BAC was found to have deleterious effects on mitochondrial functioning causing collapse of the membrane potential, promoting membrane permeabilization, inhibiting ATP synthesis, and promoting hydrogen peroxide production. In yeast cells, BAC triggered oxidative stress and mitochondrial fragmentation; its prooxidant effect can be partially prevented by the mitochondria-targeted antioxidant.

2. Materials and Methods

2.1. Chemical Reagents. Adenylate kinase, aminotriazole, Amplex Red, Ap5A, ATP, carbonylcyanide m-chlorophenylhydrazone (CCCP), cyclosporine A (CsA), EGTA, fatty acid-free BSA, glutamate, glucose-6-phosphate dehydrogenase, glycerol, hexokinase, malate, succinate, sucrose, mannitol, rotenone, NADP, phosphoenolpyruvate, pyruvate kinase, $MgCl_2$, $(NH_4)_2SO_4$, NaCl, Phenol red, and Tris were purchased from Sigma-Aldrich (USA). BAC (as a mixture of BACs with an average mol. weight of 360 and benzyldimethyldodecylammonium chloride as the prevalent species present) was from Fluka (Germany); Coomassie G-250 was from MP Biomedicals (USA); safranin O, KH_2PO_4, K_2HPO_4, KCl, and $CaCl_2$ were from Merck (Germany); MitoTracker Green FM, and H_2DCF-DA, and propidium iodide were from Life Technologies (USA). Other reagents of the highest quality available were from domestic suppliers. SkQ1 was a gift from Dr. G. A Korshunova.

2.2. Isolation of Rat Liver Mitochondria. In this study, adult (200–250 g) Wistar albino rats were used. The animal handling and mitochondria isolation were as described in [58].

2.3. Oxygen Consumption. Oxygen consumption was monitored amperometrically at 25°C using a Clark-type oxygen electrode [58]. The basic incubation medium containing 0.21 M mannitol, 0.09 M sucrose, 2 mM Tris-phosphate, pH 7.2, mitochondria (0.5 mg/ml), and either 20 mM Tris-succinate+rotenone (2 μg/mg protein) or 20 mM Tris-glutamate, 5 mM Tris-malate was supplemented with 0.5 mM EGTA. Respiratory control ratios were calculated according to [59].

2.4. Transmembrane Potential Generation ($\Delta\psi$). Potential generation on the inner mitochondrial membrane ($\Delta\psi$) was recorded as described in [58].

2.5. Swelling of Mitochondria. Swelling of mitochondria was recorded with a Varian Cary 300 Bio spectrophotometer (USA) by tracing the decrease in apparent absorbance of the mitochondrial suspensions at 540 nm [58].

2.6. Opening of the Nonspecific Ca^{2+}/Pi-Dependent Pore. Opening of the nonspecific Ca^{2+}/Pi-dependent pore (mPTP) was judged from the combination of two parameters [60], i.e., from the membrane potential depolarization and large-scale swelling of the mitochondria isolated and incubated in EGTA-free media.

2.7. ATP Synthesis by Mitochondria. ATP synthesis by rat liver mitochondria was monitored by two independent methods. The first one is based on the use of a pH-dependent dye Phenol red to follow small pH shifts during ADP conversion to ATP [61]. The basic incubation medium was supplemented with 0.5 mM EGTA, 6 μM Ap5A (the inhibitor of adenylate kinase), 25 μM Phenol red, and mitochondria (0.5 mg mitochondrial protein/ml). All stock solutions and additives were carefully adjusted to pH 7.1. Synthesis of ATP was induced by the addition of 500 μM ADP and assayed spectrophotometrically at 557/618 nm with a Beckman Coulter DU-650 spectrophotometer (USA).

The second method, being complementary to the first one, is based on the association of ATP synthesis with NADP reduction in enzymatic reactions involving NADP, hexokinase, and glucose-6-phosphate dehydrogenase. The basic incubation medium was supplemented with 0.5 mM EGTA, 6 μM Ap5A, 1 mM glucose, 1 mM NADP, hexokinase (10 IU/ml), glucose-6-phosphate dehydrogenase (3 IU/ml), and mitochondria (0.5 mg protein/ml). The synthesis of ATP was initiated by adding 100 μM ADP and monitored with a Varian Cary 300 Bio (USA) spectrophotometer at 340 nm.

2.8. Hydrogen Peroxide Production by Mitochondria. Hydrogen peroxide production by mitochondria was determined fluorometrically by measuring oxidation of Amplex Red coupled to the enzymatic reduction of H_2O_2 by horseradish peroxidase (HRP) as described in [58]. The incubation medium was supplemented with 0.5 mM EGTA, 20 mM Tris-succinate, 6 mM aminotriazole (an inhibitor of catalase), 5 μM Amplex Red, 9 U/ml horseradish peroxidase, and mitochondria (0.25 mg protein/ml). Where indicated, 1.5 μM antimycin A (an inhibitor of electron transport in complex III of the respiratory chain) and 3 μM SkQ1 were added. Fluorescence signal from a well containing all substrates and inhibitors, but not mitochondria, was subtracted as a background for every experimental condition used. Thus, any nonenzymatic effect of the inhibitors on apparent ROS production was eliminated.

2.9. Assay of Mitochondrial Protein. Mitochondrial protein was assayed by the Bradford method [62] with BSA as a standard.

2.10. Yeast Cell Cultures. In this study, we used the *Yarrowia lipolytica* strain obtained by RZ [63] and the *Dipodascus* (formerly *Endomyces*) *magnusii* yeast, strain VKM Y261. Cells were cultivated as described in [58].

2.11. ROS Determination in Yeast Cells. Production of intracellular reactive oxygen species (ROS) was detected using the nonfluorescent cell-permeating compound, 2′-7′-dichlorofluorescein diacetate (DCF-DA) as described in [58]. DCF-DA is hydrolyzed by intracellular esterases and then oxidized by ROS to a fluorescent compound, 2′-7′-dichlorofluorescein (DCF), detecting primarily hydrogen peroxide. Exponentially grown *Y. lipolytica* cells were either incubated with 10 μM BAC for 2 h or initially preincubated with 3 μM SkQ1 for 30 min and then incubated with 10 μM BAC for 2 h. All samples were rinsed with a fresh portion of growth medium and incubated with 15 μM H_2DCF-DA for 30 min. Stained cells were analyzed for DCF detection by flow cytometry with a Becton & Dickinson FACSCalibur flow cytometer (USA).

2.12. Visualization of Mitochondria in Cells. Mitochondria were stained with the 200 nM fluorescent probe MitoTracker Green FM (Life Technologies, USA) that labels mitochondria in a membrane potential-independent manner. Stained cells were observed under the Olympus BX51 fluorescence

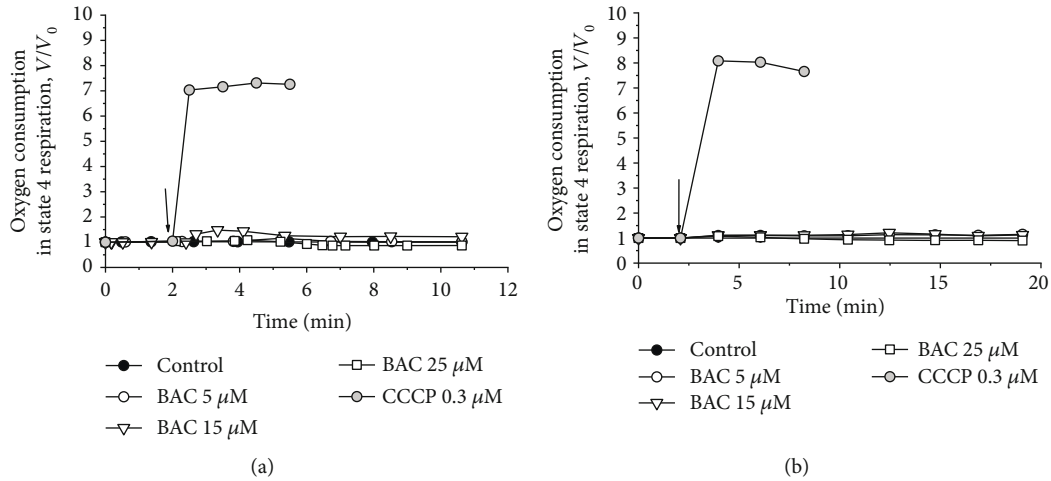

Figure 2: Effect of CCCP and varying BAC concentrations on state 4 respiration (V) of rat liver mitochondria respiring on (a) succinate or (b) glutamate+malate. First derivatives of amperometric curves are shown. The basic incubation medium was supplemented with 0.5 mM EGTA, mitochondria (0.5 mg protein/ml), and either (a) 20 mM Tris-succinate+rotenone (2 μg/mg protein) or (b) 20 mM Tris-glutamate and 5 mM Tris-malate. Additions and amounts are given on the figures. Arrows point to the addition of CCCP and varying BAC concentrations. V_0 is defined as respiratory rate in state 4 respiration before the addition of CCCP and varying BAC concentrations (24.8 or 11.2 ng-atom O/min per mg protein upon oxidation of succinate or glutamate+malate, respectively).

microscope (Japan) equipped with 100x UPlanFL Oil objective (NA 1.30). Details are given in figure legends.

2.13. Time-Lapse Microscopy. For time-lapse microscopy (see [64]), *D. magnusii* cells harvested at the exponential growth phase were washed with 50 mM PBS, pH 5.5, and stained with 200 nM MitoTracker Green FM for 30 min. Stained cells were resuspended in a fresh portion of growth medium (the control variant), exposed to 45 μM BAC, and observed under the Olympus BX51 microscope (Japan) equipped with 100x UPlanFL Oil objective (NA 1.30) for the times indicated. Images were acquired at specified intervals using Olympus DP30BW CCD camera (Japan). Images were analyzed with Icy software [65].

2.14. 3D Reconstruction of Mitochondrial Structures in D. magnusii. For 3D reconstruction, *D. magnusii* cells harvested at the exponential growth phase were incubated in a fresh portion of incubation medium (the control variant) or exposed to 45 mM BAC for 1 hour, then washed with 50 mM PBS, pH 5.5, and stained with 200 nM MitoTracker Green FM. Imaging was performed using an inverted motorized microscope Nikon Eclipse Ti-E with Perfect Focus autofocusing system (Japan). The microscopy system was equipped with 100x Apo TIRF Oil objective (NA1.49) and cooled EM-CCD camera Andor iXonDU-897E (United Kingdom) under the control of NIS-Elements 4.0 software. Serial optical sections were deconvolved using the AutoQuant blind deconvolution algorithm included in the NIS-Elements package. 3D reconstruction was performed by using Icy software [65].

2.15. Statistical Analysis. Unless otherwise specified, all experiments with isolated rat liver mitochondria were performed at least four times with consistent results. For analysis of mitochondrial morphology, at least fifty cells were examined in each trial. Data are presented as $X_{\text{mean}} \pm \text{SD}$; $n = 4$. The statistical analyses were carried out by the one-way ANOVA test.

3. Results

3.1. Characteristics of Rat Liver Mitochondria Preparations. Preparations of rat liver mitochondria used in this study met all known criteria of physiological integrity as inferred from their ability to maintain distinctive state 4–3 respiration transitions upon successive additions of ADP, high respiratory rates, high respiratory control ratios ranging from 8 to 13 upon oxidation of NAD-dependent substrates, ADP/O ratios close to the theoretically expected maxima for the substrates studied, and some additional tests including an ability to maintain the substrate-supported membrane potential at the highest possible level for a long time; stimulation of respiration in state 4 by addition of AMP instead of ADP in the Mg^{2+}-free incubation medium, which is indicative of preserving appreciable amounts of intramitochondrial Mg^{2+} and adenylate kinase largely located in the intermitochondrial space; cytochrome *c* test in evaluation of the intactness of the outer mitochondrial membrane.

3.2. Effect of BAC on Oxygen Consumption by Rat Liver Mitochondria in State 4 Respiration. At moderate concentrations, BAC only slightly and transiently stimulated oxidation of succinate (Figure 2(a)) or NAD-dependent substrates (glutamate and malate) (Figure 2(b)) in state 4 respiration. The classical anionic uncoupler CCCP increased the rate of substrate oxidation in state 4 several fold, usually to an extent comparable to the respiratory control ratio. As the effect exerted by BAC was developed with time, we displayed in the figures the first derivatives of amperometric curves of oxygen consumption. Thus, BAC did not exhibit an uncoupling activity, resembling in this respect the action

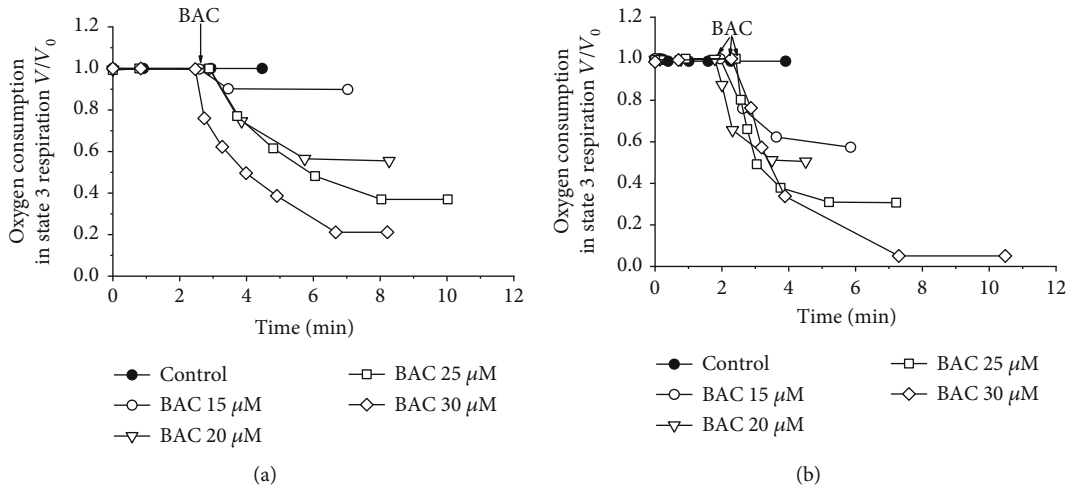

Figure 3: Inhibitory effect of varying BAC concentrations on state 3 respiration (V) of rat liver mitochondria respiring on (a) succinate or (b) glutamate+malate. First derivatives of amperometric curves are shown. The basic incubation medium was supplemented with 0.5 mM EGTA, mitochondria (0.5 mg protein/ml), and either (a) 20 mM Tris-succinate+rotenone (2 μg/mg protein) or (b) 20 mM Tris-glutamate and 5 mM Tris-malate. State 3 respiration was initiated by the addition of 0.9 mM ADP. Additions and amounts are given on the figures. Arrows point to the additions of varying BAC concentrations. V_0 is defined as respiratory rate in state 3 (in the presence of ADP) before the addition of varying BAC concentrations (172.4 or 89.8 ng-atom O/min per mg protein upon oxidation of succinate or glutamate+malate, respectively).

of other hydrophobic quaternary ammonium compounds such as decyltriethylammonium bromide (C_{10}TEA) and cetyltrimethylammonium bromide (C_{16}TMA) investigated previously [66].

3.3. Effect of BAC on Oxygen Consumption by Rat Liver Mitochondria in State 3 and Uncoupled Respiration. In the presence of ADP (in state 3 respiration), BAC inhibited oxidation of both succinate (Figure 3(a)) and NAD-dependent substrates (Figure 3(b)). In contrast, in the uncoupled state (in the presence of CCCP), BAC only slightly inhibited respiration supported by succinate or NAD-dependent substrates (not shown), suggesting that the main targets of BAC may be the translocase of adenine nucleotides or/and ATP synthase. As will be shown below, some of these assumptions proved to be justified.

3.4. BAC-Induced Depolarization of Rat Liver Mitochondria. BAC addition caused depolarization of mitochondria (Figure 4), the depolarizing effect being much stronger upon oxidation of NAD-dependent substrates (Figure 4(a), curve *1*) than in the case of succinate oxidation (Figure 4(a), curve *2*). The BAC-induced membrane depolarization was not reversed by the addition of ATP (not shown). In our previous work comprising direct trials [67], we argued that the ATP-induced recovery of the membrane potential after depolarization by a tested compound provides evidence against the membrane damage or disruption of ATP synthesis. The lack of ATP-related recoupling after the dissipation of membrane potential by BAC addition supported the view that BAC may exert a damaging effect on mitochondrial bioenergetics or even on mitochondrial membrane integrity.

3.5. BAC-Induced Opening of the mPTP in Rat Liver Mitochondria. Rat liver mitochondria isolated and suspended in EGTA-free medium exhibited spontaneous decline in the membrane potential (Figure 5(a), curve *1*) and swelling (Figure 5(b), curve *1*) presumably because of the opening of the Ca^{2+}/Pi-dependent, mildly anionic pore known as the mitochondrial permeability transition pore (mPTP) and mPTP-related unrestricted entry of osmotically active solutes into the mitochondrial matrix followed by the water uptake. These spontaneous membrane depolarization and swelling were completely inhibited in the presence of 0.5 mM EGTA or CsA (1.8 μg/mg protein) (not shown) added at zero time (Figures 5(a) and 5(b), curve *2*), thus supporting the fact that the initial spontaneous partial opening of the mPTP took place. 8 μM BAC caused collapse of the membrane potential (Figure 5(a), curve *1*) and increased the amplitude of swelling (Figure 5(b), curve *3*), which most likely reflected promotion of the mPTP opening.

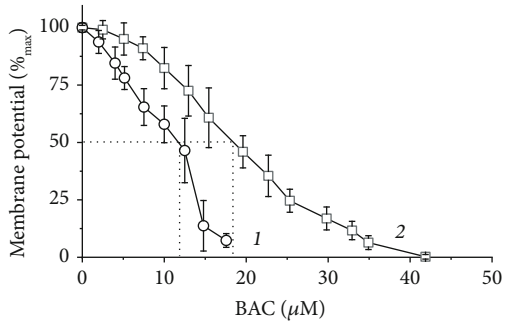

Figure 4: Membrane depolarization by BAC. The basic incubation medium was supplemented with 0.5 mM EGTA, 20 mM safranin O, mitochondria (0.5 mg protein/ml), and either 20 mM Tris-glutamate and 5 mM Tris-malate (curve *1*) or 20 mM Tris-succinate+rotenone (2 μg/mg protein) (curve *2*).

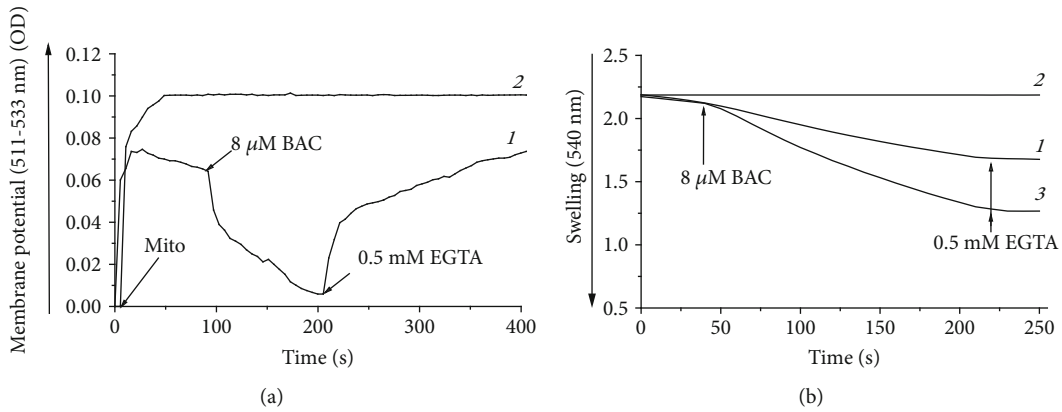

Figure 5: BAC promoted opening of the mPTP, as inferred from recording of the (a) membrane potential and (b) swelling of rat liver mitochondria isolated in EGTA-free medium. The basal incubation medium was supplemented with 20 mM Tris-succinate+rotenone (2 μg/mg protein), mitochondria (0.5 mg protein/ml), and either (a) 20 mM safranin or (b) 40 mM KCl. (a, b) Curves *1*, spontaneous depolarization (a, curve *1*) and swelling (b, curve *1*) of rat liver mitochondria; (a, b) curves *2*, the media initially contained 0.5 mM EGTA; in (a), curve *1*, depolarizing effect of 8 μM BAC and repolarization after the subsequent addition of 0.5 mM EGTA; in (b), curve *3*, promotion of mitochondrial swelling by 8 μM BAC and subsequent compression of mitochondria after the addition of 0.5 mM EGTA at the end of incubation.

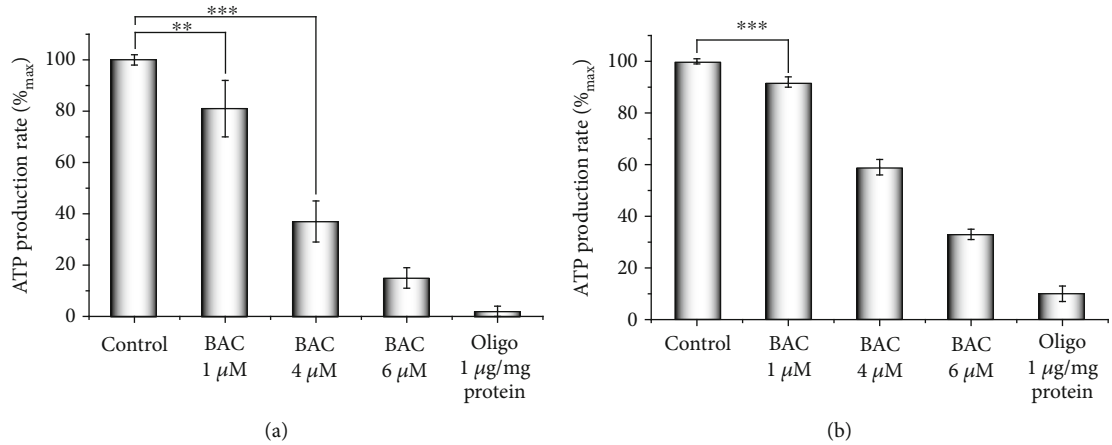

Figure 6: Inhibitory effect of BAC on ATP production by rat liver mitochondria respiring on succinate. The basal incubation medium was supplemented with 0.5 mM EGTA, 6 μM Ap5A, an inhibitor of adenylate kinase, 20 mM Tris-succinate+rotenone (2 μg/mg protein), and either (a) 25 μM Phenol red and mitochondria (0.5 mg protein/ml) or (b) 1 mM glucose, 1 mM NADP, 10 U/ml hexokinase, 3 U/ml glucose-6-phosphate dehydrogenase, and mitochondria (0.25 mg protein/ml). Where indicated, oligomycin (Oligo, 1 μg/mg protein) and varying BAC concentrations were added. The statistical analyses were carried out by the one-way ANOVA test. $^{***}p < 0.001$; $^{**}0.001 < p < 0.01$.

3.6. BAC-Induced Inhibition of ATP Synthesis by Rat Liver Mitochondria. ATP synthesis was assayed in rat liver mitochondria respiring on succinate by two independent methods (for details, see Materials and Methods) with similar results (Figures 6(a) and 6(b)). To prevent mPTP opening, the basic incubation medium was supplemented with 0.5 mM EGTA; 6 μM Ap5A, an inhibitor of adenylate kinase activity, was also added. Oligomycin, a well-known inhibitor of ATP synthesis in mitochondria, was used as a positive control. BAC was found to be a powerful inhibitor of ATP synthase sufficiently diminishing ATP synthesis even at very low concentrations not inhibiting state 3 respiration and only nominally depolarizing the membrane potential.

3.7. BAC-Induced Promotion of Hydrogen Peroxide Production by Rat Liver Mitochondria. Finally, we examined BAC effect on hydrogen peroxide production by rat liver mitochondria respiring on succinate (Figure 7). To prevent catalase activity, the medium was supplemented with 6 mM aminotriazole. Antimycin A, an inhibitor of electron transport in complex III of the respiratory chain, known to enhance hydrogen peroxide production by stimulating the reverse electron transfer, was taken as a positive control. Hydrogen peroxide production by mitochondria was almost doubled in the presence of 10 μM BAC, attaining a level comparable to that exerted by 1.5 μM antimycin A, clearly showing that BAC acted as a prooxidant.

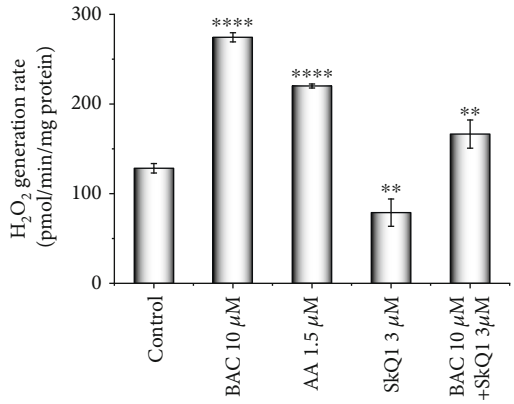

Figure 7: Hydrogen peroxide generation by rat liver mitochondria respiring on succinate. The basal incubation medium was supplemented with 0.5 mM EGTA, 20 mM Tris-succinate, 6 mM aminotriazole, 5 μM Amplex Red, horseradish peroxidase (9 IU/ml), and mitochondria (0.25 mg protein/ml). The statistical analyses were carried out by the one-way ANOVA test against control. $^{**}0.001 < p < 0.01$; $^{****}p < 0.0001$.

BAC-induced peroxide production by mitochondria was considerably diminished by SkQ1, a rechargeable mitochondria-targeted antioxidant [67].

3.8. BAC-Induced Oxidative Stress in the Y. lipolytica Yeast. Production of intracellular ROS was detected with the use of DCF (for details, see Materials and Methods). In the control experiments (Figure 8(a)), SkQ1 only marginally decreased the DCF-related fluorescence of the control cells. Exposure of exponentially grown *Y. lipolytica* cells to 10 μM BAC induced oxidative stress (Figure 8(b)), as inferred from a shift towards stronger DCF fluorescence (Figure 8(b), marked by black). The BAC-induced oxidative stress was largely prevented by SKQ1 (Figure 8(b), marked by light grey). In Figure 8(c), the data obtained are presented as diagrams.

3.9. BAC-Induced Fragmentation of Mitochondria in D. magnusii Cells. Normally, *D. magnusii* cells possess highly branched mitochondrial reticulum (Figure 9(a)). However, when cells were treated with 45 μM BAC for 1 h, disruption of the integrity of this mitochondrial reticulum (mitochondrial fragmentation) took place (Figure 9(c)). A 1 h preincubation of yeast cells with SkQ1, living mitochondrial morphology unchanged (Figure 9(b)), partially prevented BAC-induced mitochondrial fragmentation (Figure 9(d)), presumably by alleviating the oxidative stress challenge.

To gain a better insight into mitochondrial structure and dynamics in real time in single *D. magnusii* cells, we have used time-lapse microscopy (Figure 10 and Videos 1 and 2 in the Supplementary Material) and 3D reconstruction of the yeast mitochondrial system (Figure 11 and Video 3 in the Supplementary Material). Both strategies reinforced the notions that under "normal" conditions *D. magnusii* cells retained mitochondrial reticulum (Figures 10(a) and 11(a), Videos 1 and 3a in the Supplementary Material). The integrity of mitochondrial reticulum was lost when cells were exposed to 45 μM BAC (Figures 10(b) and 11(b), Videos 2 and 3b in the Supplementary Material).

4. Discussion

Over more than two decades, a large number of studies, using a variety of models, cells, and tissues, have demonstrated that BAC causes or enhances harmful consequences on the eye structures that may deeply impact patients' quality of life, compliance, or later surgical outcome (see Introduction). This situation is reinforced by the here-obtained results. Here, we showed that BAC, even at low concentrations, induced dysfunction of mitochondria, inhibiting respiration in state 3, decreasing the membrane potential, promoting opening of the mPTP, potentiating hydrogen peroxide production by mitochondria, and severely blocking synthesis of ATP. Previously, it was reported that BAC inhibited mitochondrial ATP production and oxygen consumption in human corneal epithelial cells and cells bearing LHON mutations possibly by directly targeting mitochondrial complex I [48]. However, closer examination of this paper showed that the authors used permeabilized cells as models and, more importantly, inadequate, from the point of view of bioenergetics, "mitochondrial buffer" causing high-amplitude swelling of mitochondria with all the consequences. This does not permit to consider these data as conclusive. In our approach, we applied as a model tightly coupled (high-quality) rat liver mitochondria that are a proper biosensor for assessment of drugs and specific directed agents. A comprehensive analysis of BAC effects on mitochondria showed that BAC did not exhibit an uncoupling activity (Figure 2), resembling in this respect the behaviour of other hydrophobic lipophilic quaternary ammonium compounds such as C_{10}TEA and C_{16}TMA investigated by us previously [66]. In the cited paper, these compounds, as exemplified by C_{16}TMA, were found to possess high affinity to the membrane surface (the binding energy for C_{16}TMA was equal to 48 kJ/mol), which apparently originated from its long hydrocarbon "tail," and enhanced activation energy (for C_{16}TMA, 71 kJ/mol), and hence lowered permeability through lipid bilayer, possibly due to the small size of their charged "head." Importantly, C_{10}TEA and C_{16}TMA were inactive in the BLM test (no diffusion electric potential was generated). Assuming that C_{10}TEA, C_{16}TMA, and BAC share similar properties (they are hydrophobic lipophilic quaternary ammonium compounds with screening of positive charge of lipophilic cations by bulky residues), this might explain the lack of uncoupling activity exerted by BAC (Figure 2), as well as the development of its inhibitory effect with time (Figures 2 and 3). Most probably, depolarizing activity ($\Delta\psi$ decrease) of BAC was due to its inhibitory effect on the respiratory chain (Figure 4).

The most pronounced inhibitory effect of BAC on mitochondria was revealed when testing ATP synthesis (Figure 6). It should be noted that the rate of ATP synthesis is an integral parameter, dependent not only on ATP synthase activity

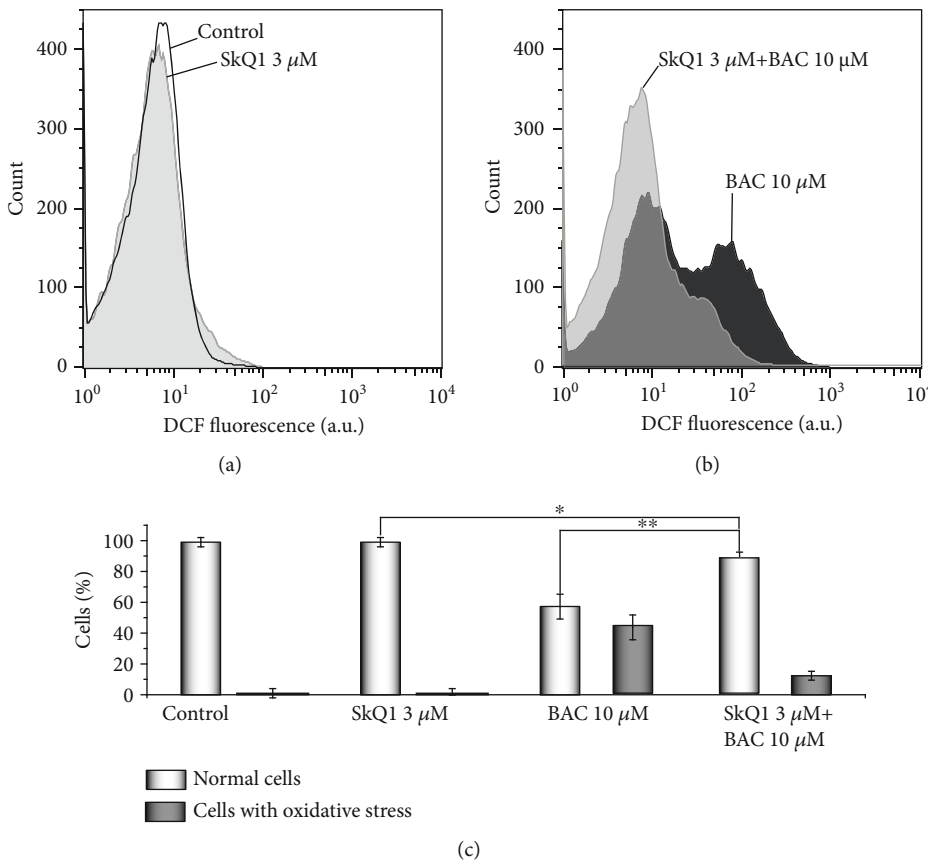

Figure 8: BAC-induced oxidative stress in the *Y. lipolytica* yeast. Exponentially grown yeast cells were either incubated with 10 μM BAC for 2 h (b, marked by black) or initially preincubated with 3 μM SkQ1 for 30 min and then incubated with 10 μM BAC for 2 h (b, marked by light grey). All samples were rinsed with a fresh portion of growth medium and incubated with 15 μM H_2DCF-DA for 30 min in the dark. Stained cells were analyzed by flow cytometry. The statistical analyses were carried out by the one-way ANOVA test. $^{**}0.001 < p < 0.01$; $^{*}0.01 < p < 0.05$.

itself but also on activity of the ADP/ATP translocase, importing ADP into the mitochondrion for ATP synthesis and exporting the synthesized ATP out of the mitochondrion for use in the cytosol. ADP/ATP translocase is the most abundant protein of the mitochondrial inner membrane, with two active centers exposed on both sites of the inner mitochondrial membrane, including the outer one [68]. The precise mechanism of inhibitory action of BAC on the translocase is unknown; this issue in the literature has been totally ignored. Keeping in mind, by analogy to C_{16}TMA, a lowered permeability of BAC through lipid bilayer, we would like to speculate that the mitochondrial ADP/ATP in the state "c conformation" (with the active center opened on the cytoplasmic side of the inner membrane) might be one of the major targets of BAC in mitochondria, most accessible for direct interaction with BAC. We are inclined to think that BAC inhibitory effect on the ADP/ATP translocase might be similar to its antimicrobial action, being associated with insertion of BAC alkyl group into the hydrophobic core of the inner mitochondrial membrane, thus disturbing the membrane and the translocase dominating in the membrane. As the ADP/ATP translocase, in addition to its normal function, forms the inner membrane channel of the mitochondrial permeability transition pore [68], a disturbance of the translocase would affect also the pore (Figure 5). BAC was found to trigger oxidative stress in mitochondria that was largely mitigated by the antioxidant SkQ1 (Figure 7). Undoubtedly, further experiments are needed to gain a better understanding of the inhibitory effects of BAC on mitochondria.

Other models utilized in this study were yeast cells with a mode of energy conservation closely similar to that of higher organisms. Yeast cells are appropriate (adequate) models for such type of investigations as they possess most of the same fundamental cellular signaling pathways that regulate metabolism, cell growth and division, organelle function, cellular homeostasis, and stress responses. Moreover, thanks to the amenability of yeast cells to both classical and advanced molecular genetic techniques, to relatively simple, cheap, and quick genetic and environmental manipulations, to the large knowledge base and data collections, high-throughput screening technologies, and functional genomics that are not possible in humans, yeasts have become valuable and prevalent eukaryotic model organisms to unravel complex fundamental intracellular mechanisms underlying human homeostasis and

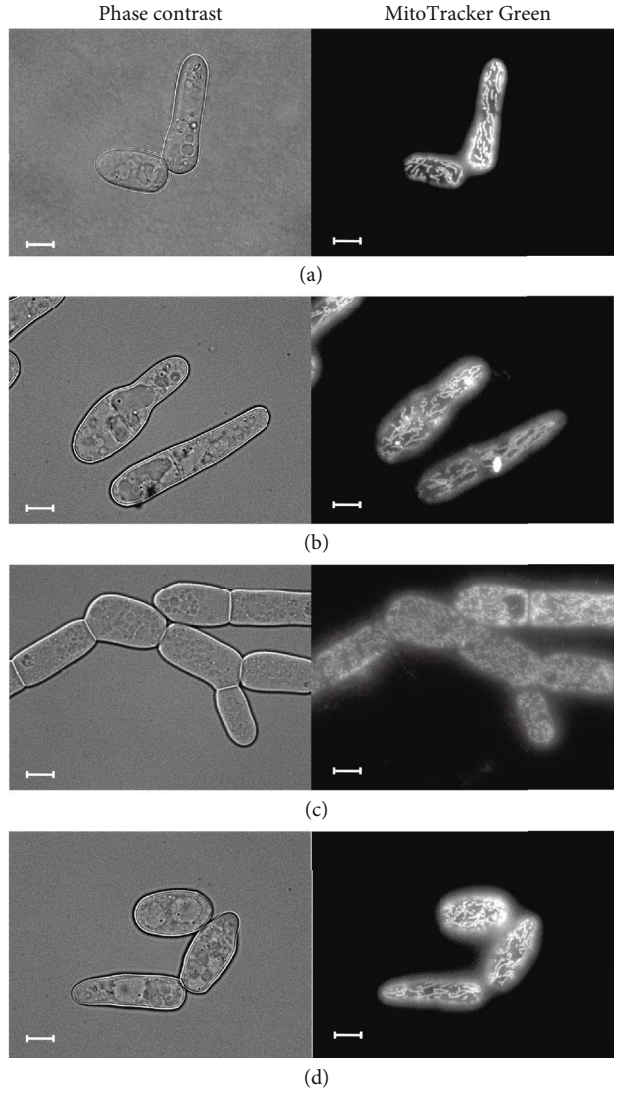

Figure 9: BAC-triggered mitochondria fragmentation in *D. magnusii* cells, the protective effect of SkQ1. Exponentially grown yeast cells were used. (a) Control cells; (b) cells were incubated with 800 nM SkQ1 for 1 h; (c) cells were incubated with 45 μM BAC for 1 h; (d) cells were preincubated with 800 nM SkQ1 for 1 h, washed in 50 mM PBS buffer, pH 5.5, suspended in a fresh portion of growth medium and then incubated with 45 μM BAC for 1 h. For visualization of mitochondria, cells were washed with 50 mM PBS, pH 5.5, and stained with 200 nM MitoTracker Green for 30 min. Scale bars are 10 μm.

pathologies. BAC in yeast cells exerted pronounced prooxidant effect (Figure 8) and triggered mitochondrial fragmentation (Figures 9–11). The latter observation deserves a special attention. Mitochondria in various eukaryotes are undergoing well-orchestrated fission and fusion [52], and this organellar dynamics, as a part of the quality control mechanism, has the power to restore the function of impaired organelles by content mixing with intact organelles. Moreover, the excessive mitochondrial fission (fragmentation), like a mitochondrial bioenergy deficit, has been documented as the earliest feature preceding appearance of known hallmarks of pathologies, in Alzheimer disease, for example [69].

Damaged action of BAC on rat liver mitochondria and yeast cells associated with its prooxidant effect can be considerably diminished by SkQ1, a mitochondria-addressed (transported exclusively in mitochondria) antioxidant (Figures 7 and 8). These promising results may be considered as a rationale for advisability of using mitochondrial-targeted antioxidants in ophthalmic formulations containing BAC and, more generally, for mitigating diseases related to oxidative stress and mitochondrial dysfunctions [70–74].

Many *in vivo* and *in vitro* studies have been developed to alleviate [29, 36, 75–80], to predict or even reverse [21] the toxic effects of BAC, to replace it for other less toxic preservatives [7, 26, 32, 81–89], or to remove BAC from formulations before the use [90].

Several findings indicate that extensive use of BAC as a disinfectant could lead to emergence of antibiotic-resistant isolates through the induction of cross-resistance, which may have important implications for both human and environmental health [21, 91–94].

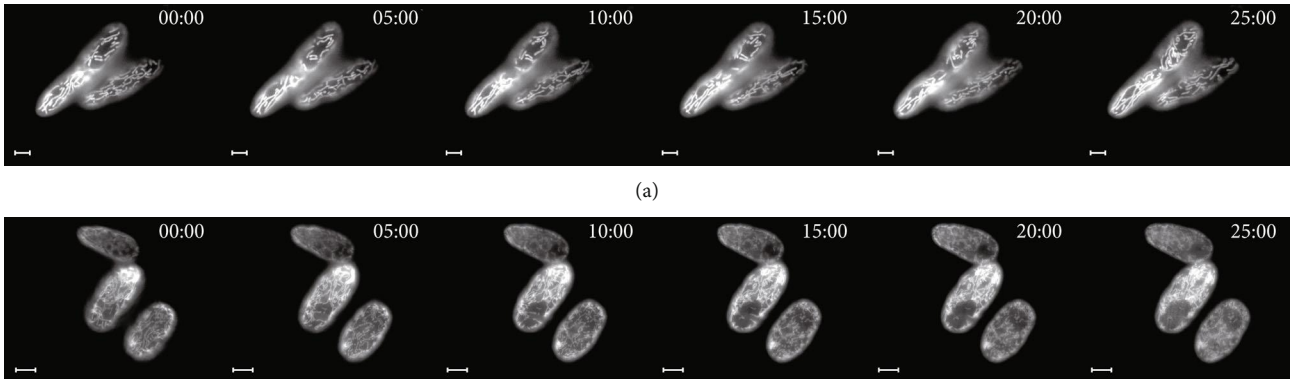

Figure 10: Time-lapse microscopy of *D. magnusii* cells. Exponentially grown yeast cells were used. For visualization of mitochondria, cells were rinsed with 50 mM PBS, pH 5.5, and then incubated with 200 nM MitoTracker Green for 30 min. (a) Control; cells were imaged for 25 min with a 30 s time interval. The full video is presented in Video 1 in the Supplementary Material. (b) Cells were incubated with 45 μM BAC; cells were imaged for 25 min with a 30 s time interval. The full video is presented in Video 2 in the Supplementary Material. Scale bars are 10 μm.

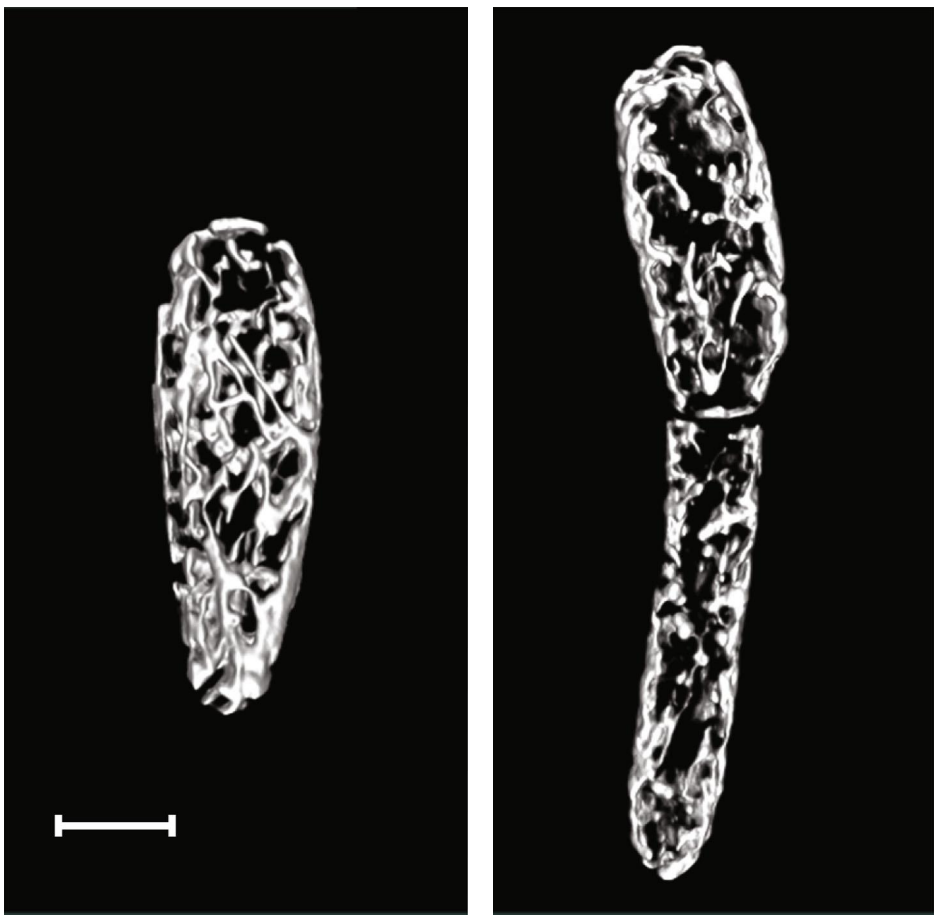

Figure 11: 3D reconstruction of mitochondrial structures in *D. magnusii* cells. Exponentially grown yeast cells were incubated in (a) fresh portion of growth medium or (b) with additionally added 45 μM BAC for 1 h. Then, cells were washed with 50 mM PBS, pH 5.5, and incubated with 200 nM MitoTracker Green for 30 min. The full video is presented in Video 3 in the Supplementary Material. Scale bars are 10 μm.

5. Conclusion

We believe that now there are more sound reasons to suggest that mitochondrial dysfunction, including lowered respiration, decreased membrane potential, opening of the mPTP, and diminished ATP production, in concert with oxidative stress and disruption of mitochondrial reticulum (mitochondrial fragmentation) may culminate BAC-induced harmful effects than this could have been assumed before [32].

Abbreviations

$\Delta\psi$:	Transmembrane electric potential difference
Ap5A:	P1,P5-di(adenosine-5′) pentaphosphate
BAC:	Benzalkonium chloride
BLM:	Bilayer planar phospholipid membrane
BSA:	Bovine serum albumin
C_{10}TEA:	Decyltriethylammonium bromide
C_{16}TMA:	Cetyltrimethylammonium bromide
CCCP:	Carbonylcyanide m-chlorophenylhydrazone
CsA:	Cyclosporine A
DCF-DA:	2′,7′-Dichlorodihydrofluorescein diacetate
EGTA:	Ethylene glycol-bis(aminoethyl ether) N,N,N′, N′-tetraacetic acid
mPTP:	Ca^{2+}/Pi-dependent mitochondrial permeability transition pore
Oligo:	Oligomycin
PI:	Propidium iodide
ROS:	Reactive oxygen species
SkQ1:	10-(6′-Plastoquinonyl)decyltriphenylphosphonium.

Data Availability

The data used to support the findings of this study are available from the corresponding author upon request.

Conflicts of Interest

The authors declare that the research was conducted in the absence of any commercial or financial relationships that could be construed as a potential conflict of interest.

Acknowledgments

The authors are grateful to Academician V.P. Skulachev for stimulating discussions and to Dr. G.A. Korshunova for providing SkQ1. The measurements were carried out on the equipment of the Shared-Access Equipment Centre "Industrial Biotechnology" of Federal Research Center "Fundamentals of Biotechnology" Russian Academy of Sciences. Microscopy facilities in A.N. Belozersky Institute were funded by the Moscow State University Development Program (PNR 5.13). Studies were partially supported by the Ministry of Science and Higher Education of the Russian Federation (grant no. 0104-2019-0013). The experiments presented in Figures 2–7 were supported by the Russian Foundation for Basic Research (grant no. 19-34-90165) and by the Russian Academy of Sciences (program "Postgenomic Technologies and Prospects of Solving the Problems in Biomedicine" AAAA-A19-119120490065-0); the experiments presented in Figures 8–11 were supported by the Russian Science Foundation (grant no. 14-24-00107).

Supplementary Materials

Supplementary 1. Video 1. Time-lapse microscopy of *D. magnusii* control cells. Yeast cells were grown as described in Materials and Methods. For visualization of mitochondria, cells were rinsed by 50 mM PBS, pH 5.5, and then incubated with 200 nM MitoTracker Green for 30 min. Cells were imaged for 25 min with a 30 s time interval. Scale bars are 10 μm.

Supplementary 2. Video 2. Time-lapse microscopy of *D. magnusii* cells incubated with 45 μM BAC. Yeast cells were grown as described in Materials and Methods. For visualization of mitochondria, cells were rinsed by 50 mM PBS, pH 5.5, and then incubated with 200 nM MitoTracker Green for 30 min. Cells were imaged for 25 min with a 30 s time interval. Scale bars are 10 μm.

Supplementary 3. Video 3. 3D reconstruction of mitochondrial structures in *D. magnusii* cells. Exponentially grown yeast cells were incubated in a fresh portion of growth medium (a) or with additionally added 45 μM BAC (b) for 1 h. Then, cells were washed by 50 mM PBS, pH 5.5, and incubated with 200 nM MitoTracker Green for 30 min. Scale bars are 10 μm.

References

[1] M. A. Safwat, G. M. Soliman, D. Sayed, and M. A. Attia, "Gold nanoparticles capped with benzalkonium chloride and poly (ethylene imine) for enhanced loading and skin permeability of 5-fluorouracil," *Drug Development and Industrial Pharmacy*, vol. 43, no. 11, pp. 1780–1791, 2017.

[2] S. C. Antunes, B. Nunes, S. Rodrigues, R. Nunes, J. Fernandes, and A. T. Correia, "Effects of chronic exposure to benzalkonium chloride in Oncorhynchus mykiss: cholinergic neurotoxicity, oxidative stress, peroxidative damage and genotoxicity," *Environmental Toxicology and Pharmacology*, vol. 45, pp. 115–122, 2016.

[3] C. Ferreira, A. M. Pereira, M. C. Pereira, L. F. Melo, and M. Simoes, "Physiological changes induced by the quaternary ammonium compound benzyldimethyldodecylammonium chloride on Pseudomonas fluorescens," *The Journal of Antimicrobial Chemotherapy*, vol. 66, no. 5, pp. 1036–1043, 2011.

[4] B. Brycki, I. Malecka, A. Kozirog, and A. Otlewska, "Synthesis, structure and antimicrobial properties of novel benzalkonium chloride analogues with pyridine rings," *Molecules*, vol. 22, no. 1, p. 130, 2017.

[5] M. Gholamrezazadeh, M. R. Shakibaie, F. Monirzadeh, S. Masoumi, and Z. Hashemizadeh, "Effect of nano-silver, nano-copper, deconex and benzalkonium chloride on biofilm formation and expression of transcription regulatory quorum sensing gene (rh1R) in drug-resistance Pseudomonas aeruginosa burn isolates," *Burns*, vol. 44, no. 3, pp. 700–708, 2018.

[6] E. G. Romanowski, K. A. Yates, R. M. Q. Shanks, and R. P. Kowalski, "Benzalkonium chloride demonstrates concentration-dependent antiviral activity against adenovirus *in vitro*," *Journal*

of Ocular Pharmacology and Therapeutics, vol. 35, no. 5, pp. 311–314, 2019.

[7] D. W. Steven, P. Alaghband, and K. S. Lim, "Preservatives in glaucoma medication," *The British Journal of Ophthalmology*, vol. 102, no. 11, pp. 1497–1503, 2018.

[8] J. R. Lechien, P. Costa de Araujo, L. G. De Marrez, J. L. Halloy, M. Khalife, and S. Saussez, "Contact allergy to benzalkonium chloride in patients using a steroid nasal spray: a report of 3 cases," *Ear, Nose, & Throat Journal*, vol. 97, no. 1-2, pp. E20–e22, 2018.

[9] S. Prabhakaran, M. Abu-Hasan, and L. Hendeles, "Benzalkonium chloride: a bronchoconstricting preservative in continuous albuterol nebulizer solutions," *Pharmacotherapy*, vol. 37, no. 5, pp. 607–610, 2017.

[10] S. L. Gulley, S. M. Baltzley, A. D. Junkins et al., "Sterility and stability testing of preservative-free albuterol," *Journal of Pediatric Pharmacology and Therapeutics*, vol. 24, no. 1, pp. 53–57, 2019.

[11] S. W. Bondurant, C. M. Duley, and J. W. Harbell, "Demonstrating the persistent antibacterial efficacy of a hand sanitizer containing benzalkonium chloride on human skin at 1, 2, and 4 hours after application," *American Journal of Infection Control*, vol. 47, no. 8, pp. 928–932, 2019.

[12] O. Ryu, B. K. Park, M. Bang et al., "Effects of several cosmetic preservatives on ROS-dependent apoptosis of rat neural progenitor cells," *Biomolecules & Therapeutics*, vol. 26, no. 6, pp. 608–615, 2018.

[13] X. Chen, D. A. Sullivan, A. G. Sullivan, W. R. Kam, and Y. Liu, "Toxicity of cosmetic preservatives on human ocular surface and adnexal cells," *Experimental Eye Research*, vol. 170, pp. 188–197, 2018.

[14] S. M. Choi, T. H. Roh, D. S. Lim, S. Kacew, H. S. Kim, and B. M. Lee, "Risk assessment of benzalkonium chloride in cosmetic products," *Journal of Toxicology and Environmental Health Part B: Critical Reviews*, vol. 21, no. 1, pp. 8–23, 2018.

[15] M. Bilal and H. M. N. Iqbal, "An insight into toxicity and human-health-related adverse consequences of cosmeceuticals – A review," *Science of The Total Environment*, vol. 670, pp. 555–568, 2019.

[16] A. Comba, T. Maravic, L. Valente et al., "Effect of benzalkonium chloride on dentin bond strength and endogenous enzymatic activity," *Journal of Dentistry*, vol. 85, pp. 25–32, 2019.

[17] A. Ozturk and A. Kalkanci, "Investigation of antifungal activities of some disinfectants on Candida albicans," *Mikrobiyoloji Bülteni*, vol. 52, no. 4, pp. 376–389, 2018.

[18] C. Baudouin, A. Denoyer, N. Desbenoit, G. Hamm, and A. Grise, "In vitro and in vivo experimental studies on trabecular meshwork degeneration induced by benzalkonium chloride (an American Ophthalmological Society thesis)," *Transactions of the American Ophthalmological Society*, vol. 110, pp. 40–63, 2012.

[19] Y. H. Kim, J. C. Jung, S. Y. Jung, S. Yu, K. W. Lee, and Y. J. Park, "Comparison of the efficacy of fluorometholone with and without benzalkonium chloride in ocular surface disease," *Cornea*, vol. 35, no. 2, pp. 234–242, 2016.

[20] H. Ji, Y. Zhu, Y. Zhang et al., "The effect of dry eye disease on scar formation in rabbit glaucoma filtration surgery," *International Journal of Molecular Sciences*, vol. 18, no. 6, p. 1150, 2017.

[21] M. L. Fernandez Marquez, M. J. Grande Burgos, M. C. Lopez Aguayo, R. Perez Pulido, A. Galvez, and R. Lucas, "Characterization of biocide-tolerant bacteria isolated from cheese and dairy small-medium enterprises," *Food Microbiology*, vol. 62, pp. 77–81, 2017.

[22] C. Portal, V. Gouyer, F. Gottrand, and J. L. Desseyn, "Preclinical mouse model to monitor live Muc5b-producing conjunctival goblet cell density under pharmacological treatments," *PLoS One*, vol. 12, no. 3, article e0174764, 2017.

[23] J. A. P. Gomes, D. T. Azar, C. Baudouin et al., "TFOS DEWS II iatrogenic report," *The Ocular Surface*, vol. 15, no. 3, pp. 511–538, 2017.

[24] P. Fogagnolo, G. Torregrossa, L. Tranchina et al., "Tear film osmolarity, ocular surface disease and glaucoma: a review," *Current Medicinal Chemistry*, vol. 26, no. 22, pp. 4241–4252, 2019.

[25] G. Roberti, L. Tanga, G. Manni et al., "Tear film, conjunctival and corneal modifications induced by glaucoma treatment," *Current Medicinal Chemistry*, vol. 26, no. 22, pp. 4253–4261, 2019.

[26] K. Walsh and L. Jones, "The use of preservatives in dry eye drops," *Clinical Ophthalmology*, vol. 13, pp. 1409–1425, 2019.

[27] Q. Yang, Y. Zhang, X. Liu, N. Wang, Z. Song, and K. Wu, "A comparison of the effects of benzalkonium chloride on ocular surfaces between C57BL/6 and BALB/c mice," *International Journal of Molecular Sciences*, vol. 18, no. 3, p. 509, 2017.

[28] E. Warcoin, C. Clouzeau, C. Roubeix et al., "Hyperosmolarity and benzalkonium chloride differently stimulate inflammatory markers in conjunctiva-derived epithelial cells in vitro," *Ophthalmic Research*, vol. 58, no. 1, pp. 40–48, 2017.

[29] K. G. Boboridis, N. Kozeis, and A. G. Konstas, "Revisiting ocular allergy: evaluating symptoms, benzalkonium chloride and efficacy of topical ketotifen 0.025," *Ocular Immunology and Inflammation*, pp. 1–3, 2019.

[30] A. S. Andrade, T. B. Salomon, C. S. Behling et al., "Alpha-lipoic acid restores tear production in an animal model of dry eye," *Experimental Eye Research*, vol. 120, pp. 1–9, 2014.

[31] C. Baudouin, "Ocular surface and external filtration surgery: mutual relationships," *Developments in Ophthalmology*, vol. 59, pp. 67–79, 2017.

[32] C. Debbasch, F. Brignole, P. J. Pisella, J. M. Warnet, P. Rat, and C. Baudouin, "Quaternary ammoniums and other preservatives' contribution in oxidative stress and apoptosis on Chang conjunctival cells," *Investigative Ophthalmology & Visual Science*, vol. 42, no. 3, pp. 642–652, 2001.

[33] F. Brignole-Baudouin, N. Desbenoit, G. Hamm et al., "A new safety concern for glaucoma treatment demonstrated by mass spectrometry imaging of benzalkonium chloride distribution in the eye, an experimental study in rabbits," *PLoS One*, vol. 7, no. 11, article e50180, 2012.

[34] M. Bouchemi, C. Roubeix, K. Kessal et al., "Effect of benzalkonium chloride on trabecular meshwork cells in a new in vitro 3D trabecular meshwork model for glaucoma," *Toxicology In Vitro*, vol. 41, pp. 21–29, 2017.

[35] A. Izzotti, S. La Maestra, R. T. Micale, M. G. Longobardi, and S. C. Sacca, "Genomic and post-genomic effects of antiglaucoma drugs preservatives in trabecular meshwork," *Mutation Research*, vol. 772, pp. 1–9, 2015.

[36] J. Moon, J. H. Ko, C. H. Yoon, M. K. Kim, and J. Y. Oh, "Effects of 20% human serum on corneal epithelial toxicity induced by benzalkonium chloride: in vitro and clinical studies," *Cornea*, vol. 37, no. 5, pp. 617–623, 2018.

[37] M. George, S. V. Joshi, E. Concepcion, and H. Lee, "Paradoxical bronchospasm from benzalkonium chloride (BAC) preservative in albuterol nebulizer solution in a patient with acute severe asthma. A case report and literature review of airway effects of BAC," *Respiratory Medicine Case Reports*, vol. 21, pp. 39–41, 2017.

[38] F. Tamer, E. Koc, T. Gun, and C. Ergin, "Nasal mucosal dysplasia induced by topical corticosteroids with benzalkonium chloride," *Indian Dermatology Online Journal*, vol. 9, no. 2, pp. 126-127, 2018.

[39] A. B. Wentworth, J. A. Yiannias, M. D. Davis, and J. M. Killian, "Benzalkonium chloride: a known irritant and novel allergen," *Dermatitis*, vol. 27, no. 1, pp. 14–20, 2016.

[40] J. Isaac and P. L. Scheinman, "Benzalkonium chloride: an irritant and sensitizer," *Dermatitis*, vol. 28, no. 6, pp. 346–352, 2017.

[41] A. J. Robinson, R. S. Foster, A. R. Halbert, E. King, and D. Orchard, "Granular parakeratosis induced by benzalkonium chloride exposure from laundry rinse aids," *The Australasian Journal of Dermatology*, vol. 58, no. 3, pp. e138–e140, 2017.

[42] K. M. Hines, J. Herron, and L. Xu, "Assessment of altered lipid homeostasis by HILIC-ion mobility-mass spectrometry-based lipidomics," *Journal of Lipid Research*, vol. 58, no. 4, pp. 809–819, 2017.

[43] J. M. Herron, K. M. Hines, H. Tomita, R. P. Seguin, J. Y. Cui, and L. Xu, "Multi-omics investigation reveals benzalkonium chloride disinfectants alter sterol and lipid homeostasis in the mouse neonatal brain," *Toxicological Sciences*, vol. 171, no. 1, pp. 32–45, 2019.

[44] S. Forbes, N. Morgan, G. J. Humphreys, A. Amezquita, H. Mistry, and A. J. McBain, "Loss of function in *Escherichia coli* exposed to environmentally relevant concentrations of benzalkonium chloride," *Applied and Environmental Microbiology*, vol. 85, no. 4, 2019.

[45] H. Jeon, D. Kim, J. Yoo, and S. Kwon, "Effects of benzalkonium chloride on cell viability, inflammatory response, and oxidative stress of human alveolar epithelial cells cultured in a dynamic culture condition," *Toxicology In Vitro*, vol. 59, pp. 221–227, 2019.

[46] Y. Uchino, T. Kawakita, M. Miyazawa et al., "Oxidative stress induced inflammation initiates functional decline of tear production," *PLoS One*, vol. 7, no. 10, article e45805, 2012.

[47] H. Onouchi, T. Ishii, M. Miyazawa et al., "Mitochondrial superoxide anion overproduction inTet-mev-1Transgenic mice accelerates age-dependent corneal cell dysfunctions," *Investigative Ophthalmology & Visual Science*, vol. 53, no. 9, pp. 5780–5787, 2012.

[48] S. Datta, C. Baudouin, F. Brignole-Baudouin, A. Denoyer, and G. A. Cortopassi, "The eye drop preservative benzalkonium chloride potently induces mitochondrial dysfunction and preferentially affects LHON mutant cells," *Investigative Ophthalmology & Visual Science*, vol. 58, no. 4, pp. 2406–2412, 2017.

[49] S. Datta, G. He, A. Tomilov, S. Sahdeo, M. S. Denison, and G. Cortopassi, "In VitroEvaluation of mitochondrial function and estrogen signaling in cell lines exposed to the antiseptic cetylpyridinium chloride," *Environmental Health Perspectives*, vol. 125, no. 8, article 087015, 2017.

[50] R. A. Zviagil'skaia, V. A. Zelenshchikova, L. A. Ural'skaia, and A. V. Kotel'nikova, "Respiratory system of Endomyces magnusii. Properties of mitochondria from cells grown on glycerol," *Biokhimiia*, vol. 46, no. 1, pp. 3–10, 1981.

[51] E. N. Andreishcheva, M. I. M. Soares, and R. A. Zvyagilskaya, "Energy metabolism of Candida (Yarrowia) lipolytica yeast under non-stressed and salt-stressed conditions," *Russian Journal of Plant Physiology*, vol. 44, pp. 657–664, 1997.

[52] A. G. Rogov, A. P. Ovchenkova, T. N. Goleva, I. I. Kireev, and R. A. Zvyagilskaya, "New yeast models for studying mitochondrial morphology as affected by oxidative stress and other factors," *Analytical Biochemistry*, vol. 552, pp. 24–29, 2018.

[53] S. Verbandt, B. P. A. Cammue, and K. Thevissen, "Yeast as a model for the identification of novel survival-promoting compounds applicable to treat degenerative diseases," *Mechanisms of Ageing and Development*, vol. 161, Part B, pp. 306–316, 2017.

[54] J. M. Coronas-Serna, M. Valenti, E. Del Val et al., "Modeling human disease in yeast: recreating the PI3K-PTEN-Akt signaling pathway in *Saccharomyces cerevisiae*," *International Microbiology*, 2019.

[55] A. V. Oliveira, R. Vilaca, C. N. Santos, V. Costa, and R. Menezes, "Exploring the power of yeast to model aging and age-related neurodegenerative disorders," *Biogerontology*, vol. 18, no. 1, pp. 3–34, 2017.

[56] D. Seynnaeve, M. Vecchio, G. Fruhmann et al., "Recent insights on Alzheimer's disease originating from yeast models," *International Journal of Molecular Sciences*, vol. 19, no. 7, p. 1947, 2018.

[57] B. Sampaio-Marques, W. C. Burhans, and P. Ludovico, "Yeast at the forefront of research on ageing and age-related diseases," *Progress in Molecular and Subcellular Biology*, vol. 58, pp. 217–242, 2019.

[58] T. N. Goleva, A. G. Rogov, G. A. Korshunova et al., "SkQThy, a novel and promising mitochondria-targeted antioxidant," *Mitochondrion*, vol. 49, pp. 206–216, 2019.

[59] B. Chance and G. R. Williams, "A simple and rapid assay of oxidative phosphorylation," *Nature*, vol. 175, no. 4469, pp. 1120-1121, 1955.

[60] P. Bernardi, A. Krauskopf, E. Basso et al., "The mitochondrial permeability transition from in vitro artifact to disease target," *The FEBS Journal*, vol. 273, no. 10, pp. 2077–2099, 2006.

[61] T. V. Zharova and A. D. Vinogradov, "Energy-linked binding of P_i is required for continuous steady-state proton-translocating ATP hydrolysis catalyzed by $F_o{\cdot}F_1$ ATP Synthase," *Biochemistry*, vol. 45, no. 48, pp. 14552–14558, 2006.

[62] M. M. Bradford, "A rapid and sensitive method for the quantitation of microgram quantities of protein utilizing the principle of protein-dye binding," *Analytical Biochemistry*, vol. 72, pp. 248–254, 1976.

[63] R. Zvyagilskaya, E. Andreishcheva, M. I. Soares, I. Khozin, A. Berhe, and B. L. Persson, "Isolation and characterization of a novel leaf-inhabiting osmo-, salt-, and alkali-tolerant Yarrowia lipolytica yeast strain," *Journal of Basic Microbiology*, vol. 41, no. 5, pp. 289–303, 2001.

[64] A. Kumar and M. Mendoza, "Time-lapse fluorescence microscopy of budding yeast cells," *Methods in Molecular Biology*, vol. 1369, pp. 1–8, 2016.

[65] F. de Chaumont, S. Dallongeville, N. Chenouard et al., "Icy: an open bioimage informatics platform for extended reproducible research," *Nature Methods*, vol. 9, no. 7, pp. 690–696, 2012.

[66] T. A. Trendeleva, E. I. Sukhanova, A. G. Rogov et al., "Role of charge screening and delocalization for lipophilic cation permeability of model and mitochondrial membranes," *Mitochondrion*, vol. 13, no. 5, pp. 500–506, 2013.

[67] E. I. Sukhanova, T. A. Trendeleva, and R. A. Zvyagilskaya, "Interaction of yeast mitochondria with fatty acids and mitochondria-targeted lipophilic cations," *Biochemistry*, vol. 75, no. 2, pp. 139–144, 2010.

[68] A. P. Halestrap and C. Brenner, "The adenine nucleotide translocase: a central component of the mitochondrial permeability transition pore and key player in cell death," *Current Medicinal Chemistry*, vol. 10, no. 16, pp. 1507–1525, 2003.

[69] D. M. A. Oliver and P. H. Reddy, "Molecular basis of Alzheimer's disease: focus on mitochondria," *Journal of Alzheimer's Disease*, vol. 72, no. s1, pp. S95–S116, 2019.

[70] S. S. Jankauskas, E. Y. Plotnikov, M. A. Morosanova et al., "Mitochondria-targeted antioxidant SkQR1 ameliorates gentamycin-induced renal failure and hearing loss," *Biochemistry*, vol. 77, no. 6, pp. 666–670, 2012.

[71] N. A. Muraleva, O. S. Kozhevnikova, A. A. Zhdankina et al., "The mitochondria-targeted antioxidant SkQ1 restores αB-crystallin expression and protects against AMD-like retinopathy in OXYS rats," *Cell Cycle*, vol. 13, no. 22, pp. 3499–3505, 2014.

[72] V. V. Brzheskiy, E. L. Efimova, T. N. Vorontsova et al., "Results of a multicenter, randomized, double-masked, placebo-controlled clinical study of the efficacy and safety of Visomitin eye drops in patients with dry eye syndrome," *Advances in Therapy*, vol. 32, no. 12, pp. 1263–1279, 2015.

[73] E. N. Iomdina, I. P. Khoroshilova-Maslova, O. V. Robustova et al., "Mitochondria-targeted antioxidant SkQ1 reverses glaucomatous lesions in rabbits," *Frontiers in Bioscience*, vol. 20, pp. 892–901, 2015.

[74] B. A. Feniouk and V. P. Skulachev, "Cellular and molecular mechanisms of action of mitochondria-targeted antioxidants," *Current Aging Science*, vol. 10, no. 1, pp. 41–48, 2017.

[75] H. Zhang, H. Wu, J. Yang, and J. Ye, "Sodium perbarate and benzalkonium chloride induce DNA damage in Chang conjunctival epithelial cells," *Cutaneous and Ocular Toxicology*, vol. 36, no. 4, pp. 336–342, 2017.

[76] N. Tokuda, Y. Kitaoka, A. Matsuzawa et al., "Changes in ocular surface characteristics after switching from benzalkonium chloride-preserved latanoprost to preservative-free tafluprost or benzalkonium chloride-preserved tafluprost," *Journal of Ophthalmology*, vol. 2017, Article ID 3540749, 6 pages, 2017.

[77] W. Wu, H. Jiang, X. Guo et al., "The protective role of hyaluronic acid in Cr(VI)-induced oxidative damage in corneal epithelial cells," *Journal of Ophthalmology*, vol. 2017, Article ID 3678586, 6 pages, 2017.

[78] S. di Staso, L. Agnifili, S. Cecannecchia, A. di Gregorio, and M. Ciancaglini, "*In vivo* analysis of prostaglandins-induced ocular surface and periocular adnexa modifications in patients with glaucoma," *In Vivo*, vol. 32, no. 2, pp. 211–220, 2018.

[79] S. W. Kang, K. A. Kim, C. H. Lee et al., "A standardized extract of Rhynchosia volubilis Lour. exerts a protective effect on benzalkonium chloride-induced mouse dry eye model," *Journal of Ethnopharmacology*, vol. 215, pp. 91–100, 2018.

[80] G. Hollo, A. Katsanos, K. G. Boboridis, M. Irkec, and A. G. P. Konstas, "Preservative-free prostaglandin analogs and prostaglandin/timolol fixed combinations in the treatment of glaucoma: efficacy, safety and potential advantages," *Drugs*, vol. 78, no. 1, pp. 39–64, 2018.

[81] A. Labbe, A. Pauly, H. Liang et al., "Comparison of toxicological profiles of benzalkonium chloride and polyquaternium-1: an experimental study," *Journal of Ocular Pharmacology and Therapeutics*, vol. 22, no. 4, pp. 267–278, 2006.

[82] D. Muehler, K. Sommer, S. Wennige et al., "Light-activated phenalen-1-one bactericides: efficacy, toxicity and mechanism compared with benzalkonium chloride," *Future Microbiology*, vol. 12, pp. 1297–1310, 2017.

[83] Y. Hashimoto, S. Yokoo, T. Usui, Y. Tsubota, and S. Yamagami, "High permeability and intercellular space widening with brimonidine tartrate eye drops in cultured stratified human corneal epithelial sheets," *Cornea*, vol. 37, no. 2, pp. 242–247, 2018.

[84] M. Cristaldi, M. Olivieri, G. Lupo, C. D. Anfuso, S. Pezzino, and D. Rusciano, "N-Hydroxymethylglycinate with EDTA is an efficient eye drop preservative with very low toxicity: an in vitro comparative study," *Cutaneous and Ocular Toxicology*, vol. 37, no. 1, pp. 71–76, 2018.

[85] L. Nasser, M. Rozycka, G. Gomez Rendon, and A. Navas, "Real-life results of switching from preserved to preservative-free artificial tears containing hyaluronate in patients with dry eye disease," *Clinical Ophthalmology*, vol. 12, pp. 1519–1525, 2018.

[86] T. T. Wong, T. Aung, and C. L. Ho, "Ocular surface status in glaucoma and ocular hypertension patients with existing corneal disorders switched from latanoprost 0.005% to tafluprost 0.0015%: comparison of two prostaglandin analogues with different concentrations of benzalkonium chloride," *Clinical & Experimental Ophthalmology*, vol. 46, no. 9, pp. 1028–1034, 2018.

[87] L. Tong, E. Matsuura, M. Takahashi, T. Nagano, and K. Kawazu, "Effects of anti-glaucoma prostaglandin ophthalmic solutions on cultured human corneal epithelial cells," *Current Eye Research*, vol. 44, no. 8, pp. 856–862, 2019.

[88] A. Rath, M. Eichhorn, K. Trager, F. Paulsen, and U. Hampel, "In vitro effects of benzalkonium chloride and prostaglandins on human meibomian gland epithelial cells," *Annals of Anatomy*, vol. 222, pp. 129–138, 2019.

[89] N. L. V. Lopes, C. P. B. Gracitelli, M. R. Chalita, and N. V. L. de Faria, "Ocular surface evaluation after the substitution of benzalkonium chloride preserved prostaglandin eye drops by a preservative-free prostaglandin analogue," *Medical Hypothesis, Discovery and Innovation in Ophthalmology*, vol. 8, no. 1, pp. 52–56, 2019.

[90] K. H. Hsu, K. Gupta, H. Nayaka, A. Donthi, S. Kaul, and A. Chauhan, "Multidose preservative free eyedrops by selective removal of benzalkonium chloride from ocular formulations," *Pharmaceutical Research*, vol. 34, no. 12, pp. 2862–2872, 2017.

[91] T. Yu, X. Jiang, Y. Zhang, S. Ji, W. Gao, and L. Shi, "Effect of benzalkonium chloride adaptation on sensitivity to antimicrobial agents and tolerance to environmental stresses in listeria monocytogenes," *Frontiers in Microbiology*, vol. 9, p. 2906, 2018.

[92] A. Abdelaziz, F. Sonbol, T. Elbanna, and E. El-Ekhnawy, "Exposure to sublethal concentrations of benzalkonium chloride induces antimicrobial resistance and cellular changes in *Klebsiellae pneumoniae* clinical isolates," *Microbial Drug Resistance*, vol. 25, no. 5, pp. 631–638, 2019.

[93] M. Kim, M. R. Weigand, S. Oh et al., "Widely used benzalkonium chloride disinfectants can promote antibiotic resistance," *Applied and Environmental Microbiology*, vol. 84, no. 17, 2018.

[94] B. M. P. Pereira and I. Tagkopoulos, "Benzalkonium chlorides: uses, regulatory status, and microbial resistance," *Applied and Environmental Microbiology*, vol. 85, no. 13, 2019.